Advances in Nonlinear Variational Inequalities
ISSN: 1092-910X
Vol 28 No. 7s (2025)

Chemical Reaction and Hall Current Effects on MHD Casson Fluid Flow Past an Oscillating Plate in Porous Medium.

[a]Ramesh Patoliya, [b*] Dr. Vimalkumar Gohil

[a]Research Scholar, Gujarat Technological University, Ahmedabad,

[b*] Government Engg. College, Bhavnagar

[a]Email: rkpatoliya@gmail.com, [b*] Email: vpgohil0909@gmail.com, [b*] Corresponding Author

Article History:

Received: 18-12-2024

Revised:28-1-2025

Accepted:6-2-2025

Abstract:

This paper explains the impact of a chemical reaction and the hall current on the MHD Casson fluid flow passing over an oscillating plate having a porous medium. The regulating formulas are converted through a dimensionless set of formulas. The LT and ILT techniques are adopted to find solution expressions for both the velocity u and w, temperature, and concentration profiles for the fluid. To see the impact of the wall temperature of the plate on the flow of the fluid, we solve the system of governing equations and compare the results with isothermal temperature. For the few values of different physiological attributes, the numeric amounts of the velocity profile, temperature profile, and concentration profile are plotted via graph. From the graph, it is observed that Hall Current, the Porous medium's Permeability, Radiation due to Thermal Process, and generation of Heat are helping to increase the velocity profile of the fluid flow in both directions in the presence of both the temperatures, wall and isothermal. In addition, it is observed that rotation parameter k lowers the primary velocity but helps to increase the secondary velocity.

KEYWORDS:

MHD; Casson fluid; Porous medium; Skin friction; Nusselt Number; Sherwood Number.

Nomenclature

B_0	Uniform magnetic field
ω	Phase angle
C'	Concentration

θ	Dimensionless fluid temperature
D_M	Mass diffusion coefficient
u	Primary velocity in x direction
D_T	Thermal diffusion coefficient
w	Secondary velocity in z direction
Gr	Grashof number of Thermal
C	Dimensionless concentration
Gm	Grashof number of Mass
C_p	Specific heat at constant pressure
k_1	Permeability parameter
g	Gravitational Acceleration
k_1'	Permeability of porous medium
m	Hall current
k_2'	Chemical reaction
k	Rotation parameter
Pr	Prandtl number
Kr	Chemical reaction parameter
M	Magnetic parameter
U_0	Uniform velocity of the plate
Sc	Schmidt number
T'	Fluid temperature
u'	Fluid velocity in x' direction
γ	Casson fluid parameter
w'	Fluid velocity in z' direction
Ω	Uniform angular velocity
t'	Time
t	Dimensionless time
Greek symbols:	
$\emptyset$	Porous medium's Porosity
v	Kinematic viscosity coefficient
σ	Electrical conductivity

ρ	Fluid density
β'_T	Volumetric coefficient of thermal expansion
β'_c	Volumetric coefficient of concentration expansion

1. INTRODUCTION

The research of fluid flow on a sheet (plate) has received a lot of attention from industrial and engineering operations including biological fluid movement, glass fiber production, hot rolling, rubber sheets, metallic plate cooling, wire drawing, lubricant and paint performance, plastic manufacturing, melt-spinning, aerodynamic plastic sheet extrusion, polymer extrusion, etc. over the past few decades.

Many applications in physical science and engineering discipline, such as gas powered engines, gas-cooled reactor degines, thrust systems, solar technology, hypersonic jets, spacecraft, nuclear power plants, and numerous industrial areas, arise from the influence of chemical reaction and thermal radiation on convective fluid flows.

A non-Nutonian fluid modeled and analyzed by Casson(1), Some researchers have analyzed an models on Casson fluid (2-7), The properties of mass and heat transport in MHD Casson fluid flowing across a cylinder within a wavy conduit have been observed by Afraz Hussain Majeed et al. using Method of Higher-order FEM (8), as the rotation of the plate having a remarkable impact on heat and mass transfer process on the flow of the MHD Casson fluid (9). Hence, the results on the mass, Rotation, and heat transfer effects on MHD peristaltic Casson fluid transfer across an inclined plane have been derived by N. M. Hafez et al.(10), since chemical reactions have a significant impact on Casson fluid flow, Dharmendar Reddy Yanala et al. explored the mass and heat transmission on a stretching permeable sheet with chemical reaction in a 3-D radiative flow of MHD Casson fluid and the impact of heat production and absorption and chemical reactions on dynamic magneto Casson Radiation-induced flow of nano-fluid across a non-linearly stretched Riga plate (11-12). Implications of chemical reaction and absorbed radiation combined on MHD-free convective flow of Casson fluid have been analyzed by B. V. Swarnalathamma et al.(13). In addition the impacts of thermal radiation had been observed by several researchers like Jawad Raza analyzed the effects of thermal radiation and slip on the stagnation point flow of a Casson fluid across a convective stretching sheet in MHD(14) whereas MHD thermal boundary layer Casson fluid flow across a stretching wedge that can be penetrated in the presence of convective boundary conditions and nonlinear radiation was studied by Majid Hussain et al.(15), recently MHD blood flow effects in inclined blood vessels with heat radiation using Casson fluid and Casson nanofluid flowing hydromagnetically across a stretched sheet in the presence of radiation and thermoelectric has been derived by Md. Yousuf Ali et al.(16-17), B. Narsimha Reddy and P. Maddileti obtained the results on the influence of the Joule parameter and Casson nanofluid on the variable radiative flow of MHD stretching sheet (18), Some results on thermal impacts have been derived using different techniques (19-20).

The porous medium is an important physical condition that makes a remarkable impact on the MHD Casson fluid flow, N. S. Yousef et al. observed chemical reaction impact on the flow of Casson-Williamson nano-fluid with MHD dissipative over a slick stretched sheet via a porous medium (21) whereas A finite difference analysis incorporating Joule heating and viscous

dissipation impact of radiative mixed convection MHD heat propagating via a Casson fluid past an accelerating porous plate has been derived by B. Prabhakar Reddy et al.(22), Harshad R. Patel (23) modeled and derived an remarkable results on mixed convective flow of MHD Casson fluid through a porous media having curved thermal radiation, Dolat khan et al.(24) observed heat transfer analysis of ternary hybrid Casson fluid's unstable MHD slip flow via a nonlinear stretching disk embedded in a porous media.

Influenced by the aforementioned reference work and an array of possible industrial uses of the topic, this study aims to explore the impact of Hall current and chemical reaction on MHD free convection flow via a porous media over an exponentially oscillating sheet. Therefore, this paper aims to investigate the broader issue, which involves Hall current and chemical reaction effects on MHD. This study also includes graphic representation of the influence of different flow parameters found in the governing equations. From a computational point of view, the LT and ILT approach provides a more affordable numerical solution to the problem.

2 Mathematical Formulation of the Problem:

Figure. 1 shows the geometrical representation of the problem, where x′- axis represents the plate, y′-axis is perpendicular to the plate and z'-axis is normal to both x′and y′. the rotational direction of the fluid and plate both are counterclockwise having angular velocity Ω about y′-axis.

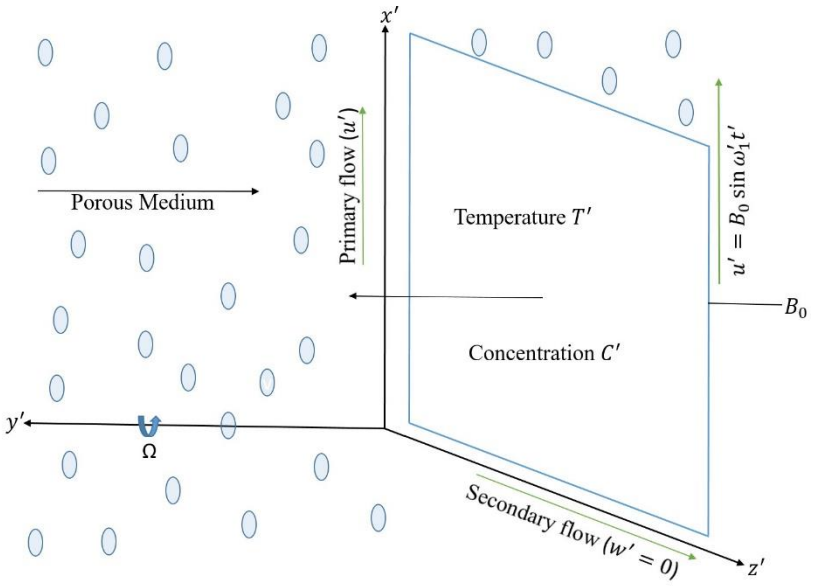

Figure 1: Geometrical representation of the stated problem

In the beginning, at the time $t' \leq 0$, the temperature of liquid and plate both are steady (say T'_∞) and the concentration of fluid is also constant (say C'_∞). When $t' > 0$, the temperature profile of the plate is quickly increased or decreased by $T'_\infty + (T'_w + T'_\infty)\frac{t'}{t_0}$ up to $t' \leq t_0$ and for $t' > t_0$, it is maintained constant(T'_w). The concentration of surface is increased directly according to $C'_\infty + (C'_w - C'_\infty)\frac{t'}{t_0}$ up to $t' \leq t_0$ and when $t' > t_0$, it remains constant(C'_w). Also the terms like ‘effects of viscous dissipation’, ‘induce magnetic’ and ‘electrical field’ are ignored. With the stated assumptions applying the Approximation of Boussinesq, the ruling formulaes are given by:

$$\rho\frac{\partial u'}{\partial t'} + 2\Omega w' = \mu B\left(1+\frac{1}{\gamma}\right)\frac{\partial^2 u'}{\partial {y'}^2} - \frac{\sigma {B_0}^2}{(1+m^2)}(u' + mw') - \frac{\mu B}{k_1'}u' + g\rho{\beta'}_T(T' - T_\infty') + g\rho{\beta'}_C(C' - C_\infty') \quad (1)$$

$$\rho\frac{\partial w'}{\partial t'} - 2\Omega u' = \mu B\left(1+\frac{1}{\gamma}\right)\frac{\partial^2 w'}{\partial {y'}^2} - \frac{\sigma {B_0}^2}{(1+m^2)}(mu' - w') - \frac{\mu B}{k_1'}u' \quad (2)$$

$$\frac{\partial T'}{\partial t'} = \frac{k}{\rho c_p}\frac{\partial^2 T'}{\partial {y'}^2} \quad (3)$$

$$\frac{\partial C'}{\partial t'} = D_M\frac{\partial^2 C'}{\partial {y'}^2} - k_2'(C' - C_\infty') \quad (4)$$

with the following beginning and boundary conditions:

$u' = 0,\ C' = C_\infty',\ w' = 0,\ T' = T_\infty'$; for $y' \geq 0,\ t' \leq 0.$

$$u' = U_0 \sin\omega' t',\ w' = 0, T' = \begin{cases} T_\infty' + (T_w' - T_\infty')\frac{t'}{t_0} & if\ 0 < t' < t_0 \\ T_w' & if\ t' \geq t_0 \end{cases},$$

$$C' = C_\infty' + (C_w' - C_\infty')\frac{t'}{t_0};\ t' \geq 0, y' = 0,$$

$u' \to 0,\ T' \to T_\infty',\ C' \to C_\infty';\ as\ y' \to \infty, t' \geq 0$ (5)

Defining the quantities without dimension like:

$$y = \frac{y'}{U_0 t_0},\ \theta = \frac{(T' - T_\infty')}{(T_w' - T_\infty')},\ u = \frac{u'}{U_0},\ C = \frac{(C' - C_\infty')}{(C_w' - C_\infty')},\ t = \frac{t'}{t_0},$$

Now, the dimensionless form of equations (1-5) becomes,

$$\frac{\partial u}{\partial t} + 2k^2 w = \left(1+\frac{1}{\gamma}\right)\frac{\partial^2 u}{\partial y^2} - \frac{M^2}{1+m^2}(u + mw) - \frac{1}{k_1}u + G_r\theta + G_m C \quad (6)$$

$$\frac{\partial w}{\partial t} - 2k^2 u = \left(1+\frac{1}{\gamma}\right)\frac{\partial^2 v}{\partial y^2} + \frac{M^2}{1+m^2}(mu - w) - \frac{1}{k_1}w \quad (7)$$

$$\frac{\partial \theta}{\partial t} = \frac{1}{Pr}\frac{\partial^2 \theta}{\partial y^2} \quad (8)$$

$$\frac{\partial C}{\partial t} = \frac{1}{s_c}\frac{\partial^2 C}{\partial y^2} - krC \quad (9)$$

with the beginning and boundary condition

$u = 0,\ w = 0,\ \theta = 0,\ C = 0,$ for $y \geq 0\ \&\ t \leq 0$

$$u = \sin(\omega t),\ w = 0,\ \theta = \begin{cases} t, 0 < t \leq 1 \\ 1, \quad t > 1 \end{cases} = tH(t) - (t-1)H(t-1),\ C = t \quad at\ y = 0\ \&\ t > 0.$$

and $u \to 0,\ w \to 0,\ \theta \to 0,\ C \to 0 \quad at\ y \to \infty\ \&\ t > 0$ (10)

In above non-dimensional equations (6-7) combined using the substitution $F = u + iw$

$$\frac{\partial F}{\partial t}+\left(\frac{M^2(1-im)}{1+m^2}+\frac{1}{k_1}-2ik^2\right)F=\left(1+\frac{1}{\gamma}\right)\frac{\partial^2 F}{\partial y^2}+G_r\theta+G_mC \quad (11)$$

$$\frac{\partial \theta}{\partial t}=\frac{1}{Pr}\frac{\partial^2\theta}{\partial y^2}$$

$$(12)\ \frac{\partial C}{\partial t}=\frac{1}{s_c}\frac{\partial^2 C}{\partial y^2}-krC$$

(13) With begining and boundary condition

$$F=0,\ \theta=0,\ C=0\ ,\ \text{for}\ y\geq 0\ \&\ t\leq 0.$$

$$F=\sin(\omega t)\ ,\ \theta=\begin{cases}t, & 0<t\leq 1\\ 1, & t>1\end{cases}=tH(t)-(t-1)H(t-1),\ C=t\ at\ y=0\ \&\ t>0$$

$$F\to 0,\ \theta\to 0,\ C\to 0\quad at\ y\to\infty\ \&\ t>0 \quad (14)$$

Where,

$$Gr=\frac{vg\beta'_T(T'_w-T'_\infty)}{U_0^3},\qquad Gm=\frac{vg\beta'_C(C'_w-C'_\infty)}{U_0^3},\qquad M=\frac{\sigma B_0^2 v}{\rho U_0^2},\qquad P_r=\frac{\rho v C_p}{k},\qquad Sc=\frac{v}{D_M},$$

$$Kr=\frac{vk_2'}{U_0^2},\qquad k_1=\frac{v\emptyset}{k_1'}.$$

3. Explanation for the said physical issue

Regulating non-dimensional formulas (11) to (13) with begining and boundary condition (14) are simplified using the Laplace and Inverse Laplace transform method and exact expression of u, w, T and C are derived.

3.1 Mathematical explanation for the stated physical issue for ramped wall T and surface C:

$$\theta(y,t)=f_2(y,t,0,a_2)-f_2(y,t-1,0,a_2)H(t-1) \quad (15)$$

$$C(y,t)=f_2(y,t,Kr,a_3) \quad (16)$$

$$F(y,t)=-\frac{1}{2i}f_3(y,t,a_1,a,iw)+\frac{1}{2i}f_3(y,t,a_1,a,-iw)+f_4(y,t)-f_4(y,t-1)H(t-1)+f_5(y,t)-f_6(y,t)+f_6(y,t-1)H(t-1)-f_7(y,t) \quad (17)$$

3.2 Mathematical explanation for the stated physical issue for isothermal T and ramped surface C:

For analyzing the impact of ramped T of the considered fluid flow, we have to match the results with isothermal T. In this situation, the begining and boundary both the conditions are the same excluding Eq. (14) that becomes $\theta=1\ at\ y=0, t\geq 0$ .We can derive the isothermal temperature $\theta(y,t)$ using Laplace transform technique.

$$\theta(y,t)=f_1(y,t,0,a_2) \quad (18)$$

$$C(y,t)=f_2(y,t,Kr,a_3) \quad (19)$$

$$F(y,t)=-\frac{1}{2i}f_3(y,t,a_1,a,iw)+\frac{1}{2i}f_3(y,t,a_1,a,-iw)+f_8(y,t)+f_5(y,t)-f_9(y,t)-f_7(y,t) \quad (20)$$

Where,

$$f_1(y,t,a,b) = L^{-1}\left(\frac{e^{-y\sqrt{\frac{s+a}{b}}}}{s}\right) = \frac{1}{2}\left[e^{-y\sqrt{\frac{a}{b}}}\, erfc\,\left(\frac{y}{2\sqrt{bt}} - \sqrt{at}\right) + e^{y\sqrt{\frac{a}{b}}}\, erfc\,\left(\frac{y}{2\sqrt{bt}} + \sqrt{at}\right)\right] \quad (21)$$

$$f_2(y,t,a,b) = L^{-1}\left(\frac{e^{-y\sqrt{\frac{s+a}{b}}}}{s^2}\right)$$

$$= \frac{1}{2}\left[\left(t - \frac{y}{2\sqrt{ab}}\right)e^{-y\sqrt{\frac{a}{b}}}\, erfc\,\left(\frac{y}{2\sqrt{bt}} - \sqrt{at}\right) + \left(t + \frac{y}{2\sqrt{ab}}\right)e^{y\sqrt{\frac{a}{b}}}\, erfc\,\left(\frac{y}{2\sqrt{bt}} + \sqrt{at}\right)\right] \quad (22)$$

$$f_3(y,t,a,b,c) = L^{-1}\left(\frac{e^{-y\sqrt{\frac{s+a}{b}}}}{(s+c)}\right)$$

$$= \frac{e^{-ct}}{2}\left[e^{-y\sqrt{\frac{1}{b}(a-c)}}\, erfc\,\left(\frac{y}{2\sqrt{b\,t}} - \sqrt{(a-c)t}\right) + e^{y\sqrt{\frac{1}{b}(a-c)}}\, erfc\,\left(\frac{y}{2\sqrt{b\,t}} + \sqrt{(a-c)t}\right)\right] \quad (23)$$

$$f_4(y,t) = a_{14}f_1(y,t,a_1,a) + a_{12}f_2(y,t,a_1,a) + a_{13}f_3(y,t,a_1,a,-a_6) \quad (24)$$

$$f_5(y,t) = a_{17}f_1(y,t,a_1,a) + a_{15}f_2(y,t,a_1,a) + a_{16}f_3(y,t,a_1,a,a_{10}) \quad (25)$$

$$f_6(y,t) = a_{14}f_1(y,t,0,a_2) + a_{12}f_2(y,t,0,a_2) + a_{13}f_3(y,t,0,a_2,-a_6) \quad (26)$$

$$f_7(y,t) = a_{17}f_1(y,t,Kr,a_3) + a_{15}f_2(y,t,Kr,a_3) + a_{16}f_3(y,t,Kr,a_3,a_{10}) \quad (27)$$

$$f_8(y,t) = a_{12}f_1(y,t,a_1,a) - a_{12}f_2(y,t,a_1,a,-a_6) \quad (28)$$

$$f_9(y,t) = a_{12}f_1(y,t,0,a_2) - a_{12}f_2(y,t,0,a_2,-a_6) \quad (29)$$

4. Formulas for τ, N_u and s_h:

The formula for $\tau = \tau_x + i\tau_z$, Nu and Sh for for both the temperature were evaluated from the equations (15-20) with the help of the expressions

$$\tau^*(y,t) = -\mu_B\left(1 + \frac{1}{\gamma}\right)\tau, \text{ Where } \tau = \frac{\partial f}{\partial y}\Big|_{y=0},\ N_u = -\left(\frac{\partial \theta}{\partial y}\right)_{y=0},\ s_h = -\left(\frac{\partial C}{\partial y}\right)_{y=0} \quad (30)$$

4.1 Solution for ramped wall T and surface C:

$$\tau(y,t) = -\frac{1}{2i}I_3(t,a_1,a,i\omega) + \frac{1}{2i}I_3(t,a_1,a,-i\omega) + I_4(t)$$

$$-I_4(t-1)H(t-1) + I_5(t) - I_6(t) + I_6(t-1)H(t-1) - I_7(t) \quad (31)$$

$$Nu = -[I_2(t,0,a_2) - I_2(t-1,0,a_2)H(t-1)] \quad (32)$$
$$Sh = -[I_2(t,Kr,a_3)] \quad (33)$$

4.2 Solution for ramped C and isothermal T:

$$\tau(y,t) = -\frac{1}{2i}I_3(t,a_1,a,i\omega) + \frac{1}{2i}I_3(t,a_1,a,-i\omega) + I_8(t) + I_5(t) - I_9(t) - I_7(t) \quad (34)$$
$$Nu = -[I_1(t,0,a_2)] \quad (35)$$
$$Sh = -[I_2(t,Kr,a_3)] \quad (36)$$

Where,

$$I_1(t,a,b) = \frac{df_1(y,t,a,b)}{dy}\Big|_{y=0} = -\sqrt{\frac{a}{b}}\ \mathrm{erf}\left(\sqrt{at}\right) - \frac{e^{-at}}{\sqrt{\pi bt}} \quad (37)$$
$$I_2(t,a,b) = \frac{df_2(y,t,a,b)}{dy}\Big|_{y=0} = -\frac{1}{\sqrt{4ab}}\ \mathrm{erf}\left(\sqrt{at}\right) - t\sqrt{\frac{a}{b}}\mathrm{erf}\left(\sqrt{at}\right) - \sqrt{\frac{t}{\pi b}}e^{-at} \quad (38)$$
$$I_3(t,a,b,c) = \frac{df_3(y,t,a,b,c)}{dy}\Big|_{y=0} = -e^{-c\,t}\sqrt{\frac{a-c}{b}}\ \mathrm{erf}\left(\sqrt{(a-c)t}\right) - \frac{e^{-at}}{\sqrt{\pi bt}} \quad (39)$$
$$I_4(t) = \frac{df_4(y,t)}{dy}\Big|_{y=0} = a_{14}I_1(t,a_1,a) + a_{12}I_2(t,a_1,a) + a_{13}I_3(t,a_1,a,-a_6) \quad (40)$$
$$I_5(t) = \frac{df_5(y,t)}{dy}\Big|_{y=0} = a_{17}I_1(t,a_1,a) + a_{15}I_2(t,a_1,a) + a_{16}I_3(t,a_1,a,a_{10}) \quad (41)$$
$$I_6(t) = \frac{df_6(y,t)}{dy}\Big|_{y=0} = a_{14}I_1(t,0,a_2) + a_{12}I_2(t,0,a_2) + a_{13}I_3(t,0,a_2,-a_6) \quad (42)$$
$$I_7(t) = \frac{df_7(y,t)}{dy}\Big|_{y=0} = a_{17}I_1(t,Kr,a_3) + a_{15}I_2(t,Kr,a_3) + a_{16}I_3(t,Kr,a_3,a_{10}) \quad (43)$$
$$I_8(t) = \frac{df_8(y,t)}{dy}\Big|_{y=0} = a_{12}I_1(t,a_1,a) - a_{12}I_2(t,a_1,a,-a_6) \quad (44)$$
$$I_9(t) = \frac{df_9(y,t)}{dy}\Big|_{y=0} = a_{12}I_1(t,0,a_2) - a_{12}I_2(t,0,a_2,-a_6) \quad (45)$$

5. Observation and Analysis

The Impact of various physical conditions like m-Hall current effect, K-rotation, M-magnetic field, k_1-porous medium's permeability, γ -Casson fluid parameter, Kr-reaction of chemical, Nr and H on the fluid flow are observed, the various values of u, w, T and C are computed from the exact solutions and described in both thermal cases (Ramped Wall Temperature and Isothermal Temperature) were presented via chart.

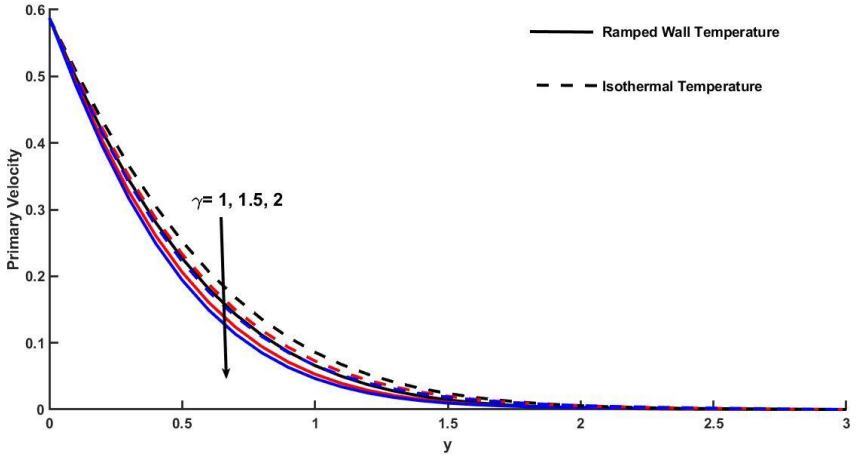

Figure 2: u on various weights of γ γ has a negative impact on u.

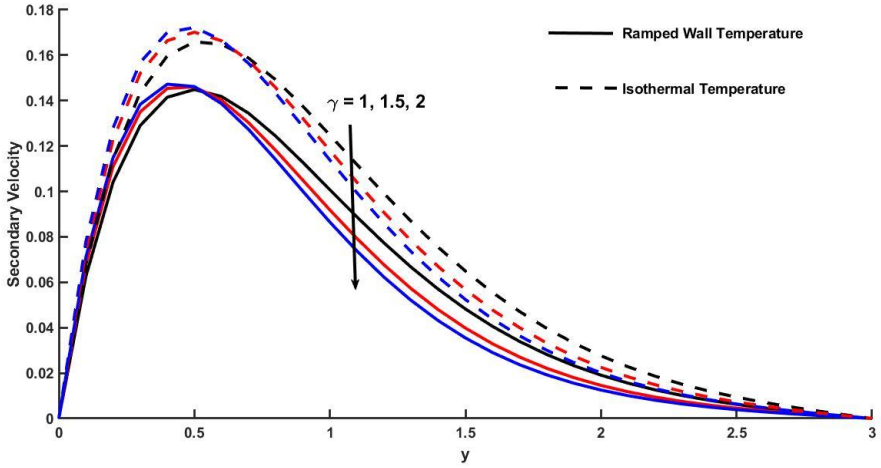

Figure 3: w on various weights of γ γ has a negative impact on w.

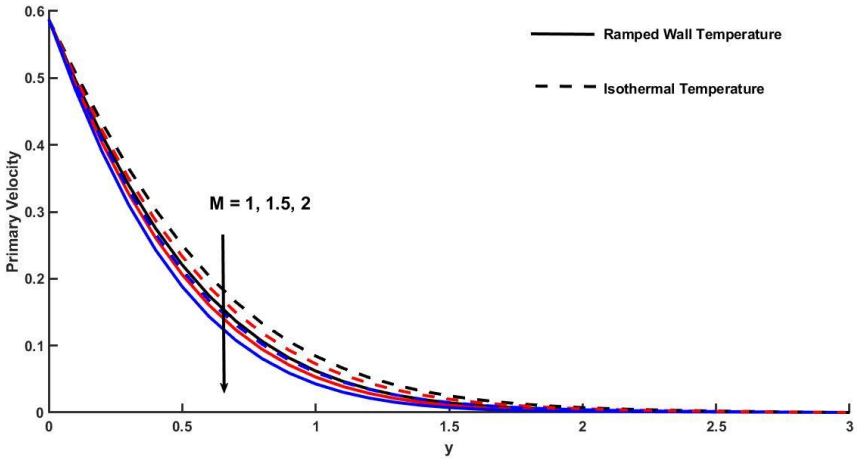

Figure 4: u on various weights of M u is decreasing as M increasing.

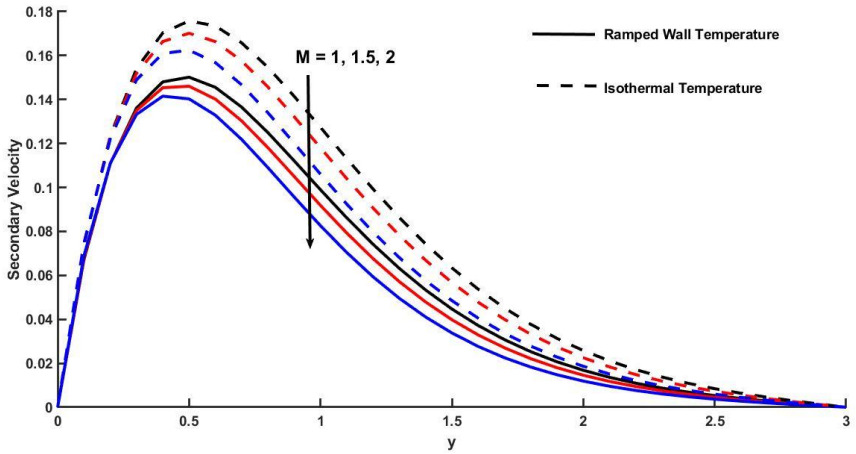

Figure 5: w on various weights of M w is decreasing as M increasing.

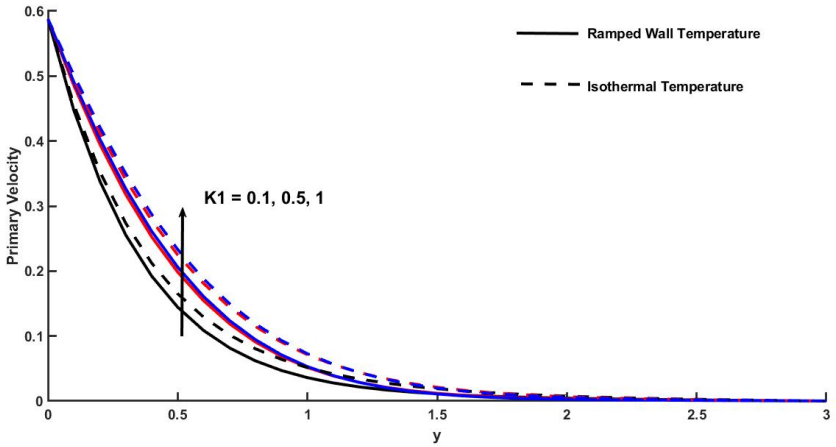

Figure 6: u on various weights of k_1 u is increasing with the increment for the values of k_1.

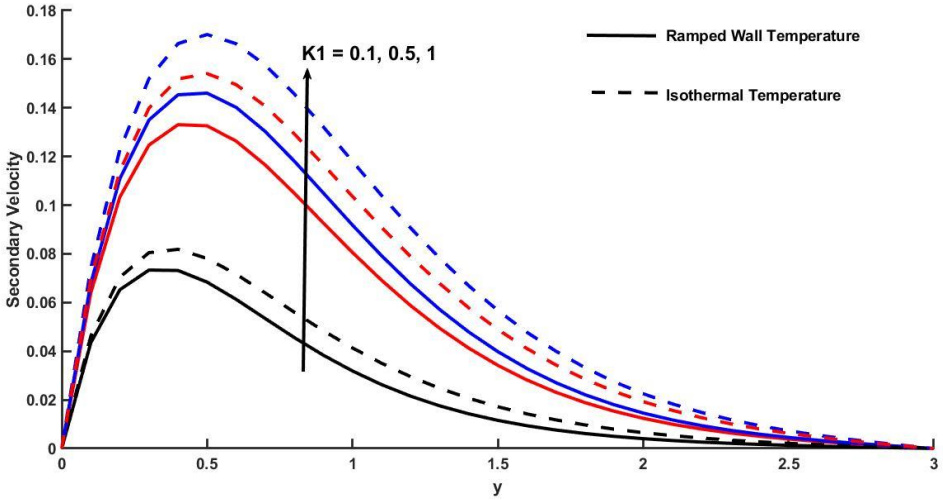

Figure 7: w on various weights of k_1. w is increasing with the increment for the values of k_1.

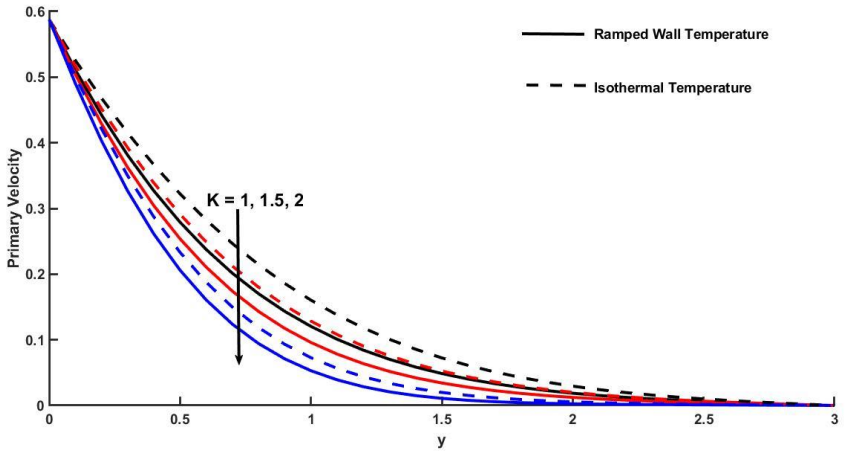

Figure 8: u on various weights of K The movement of u and K are same.

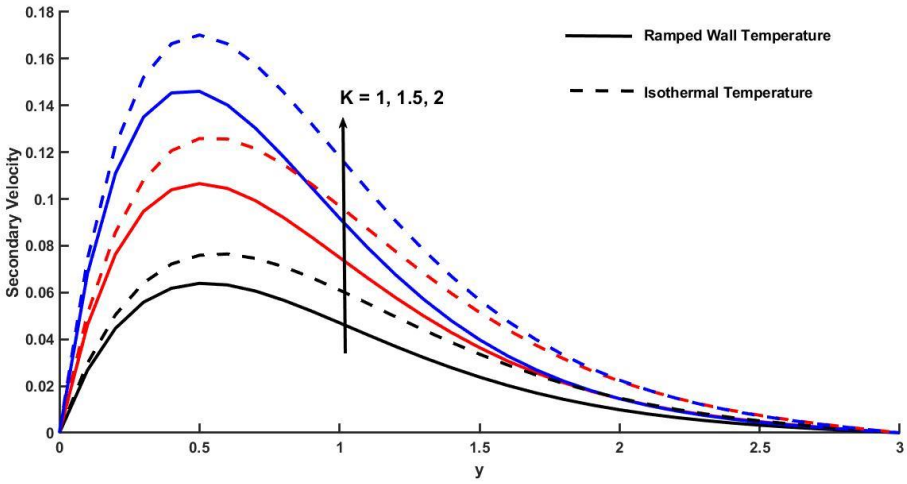

Figure 9: w on various weights of K The movement of w and K are same.

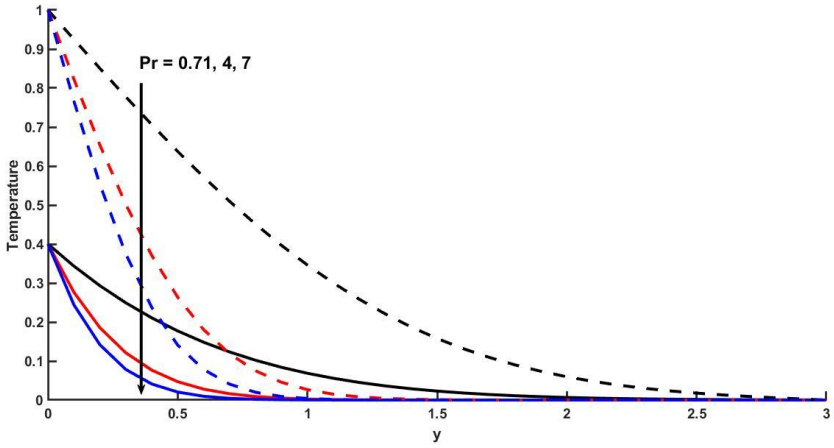

Figure 10: θ on various weights of Pr θ going down as good as increasing values of Pr.

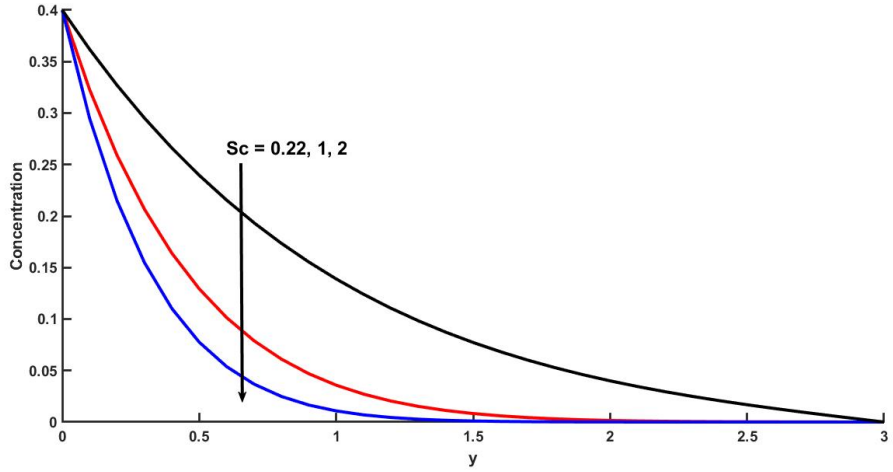

Figure 11: C on various weights of Sc Concentration profile of the fluid and Sc are negatively correlated.

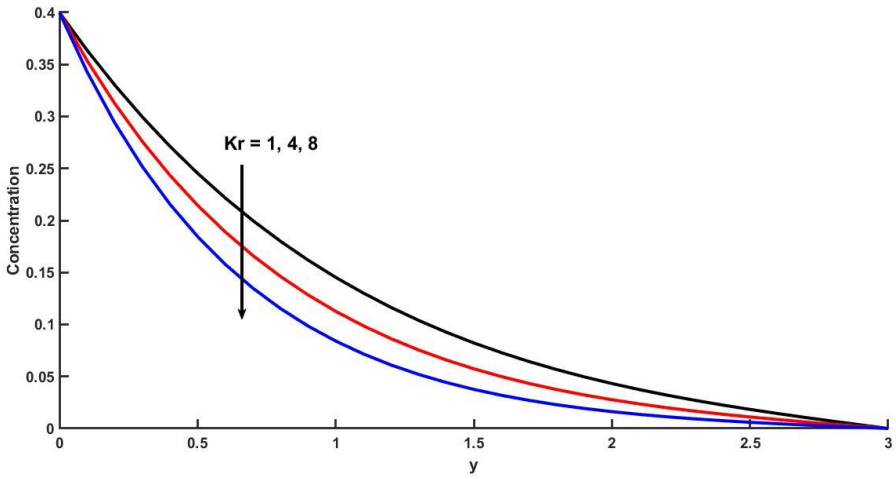

Figure 12: C on various weights of Kr Concentration profile of the fluid getting down as we increase the values of Kr.

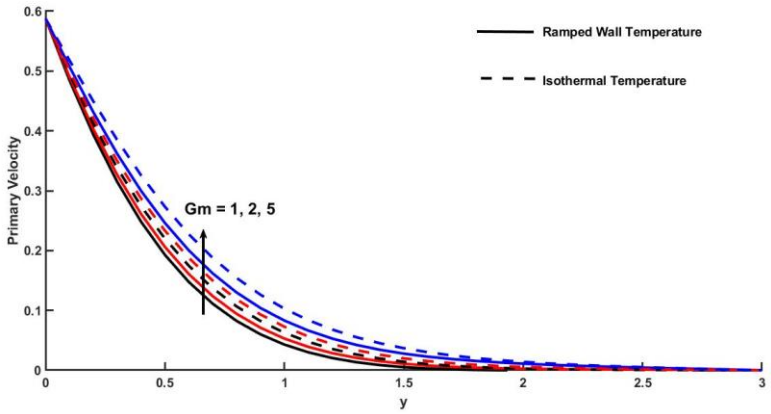

Figure 13: u on various weights of Gm Gm have the positive impact on u.

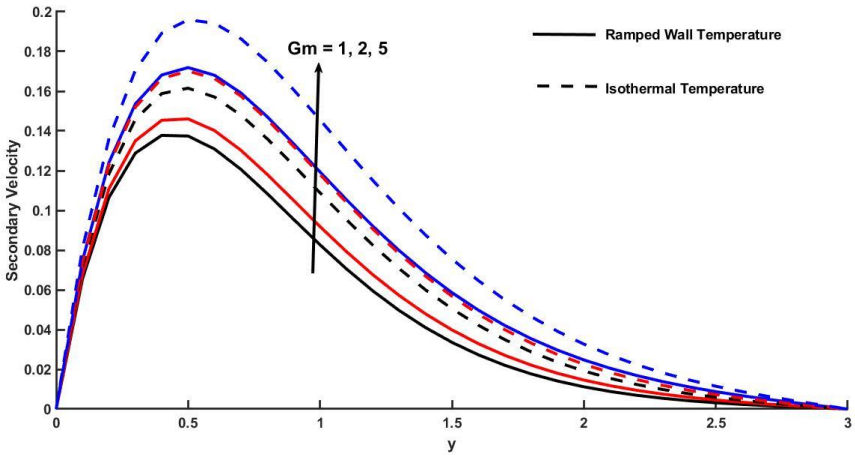

Figure 14: w on various weights of Gm Gm have the positive impact on the fluid's Secondary velocity profile

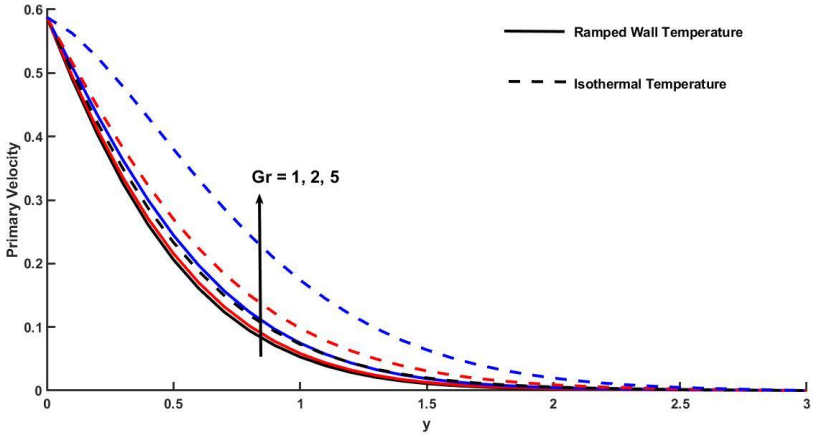

Figure 15: u on various weights of Gr Fluid's primary velocity profile have positive impact of Gr.

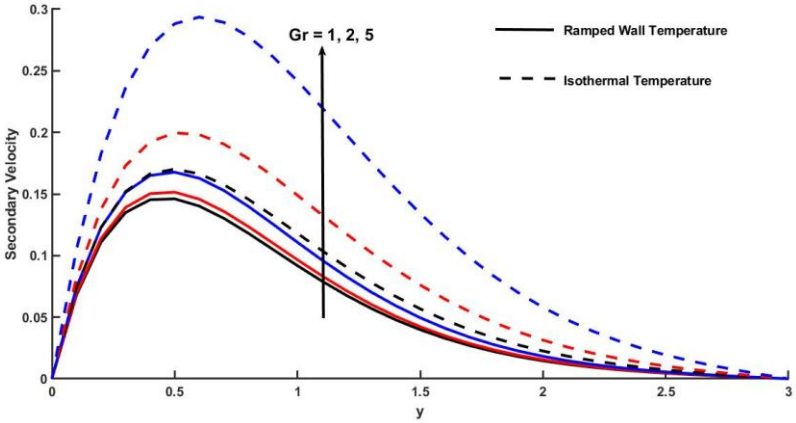

Figure 16: w on various weights of Gr Fluid's secondary velocity profile and Gr are positively correlated.

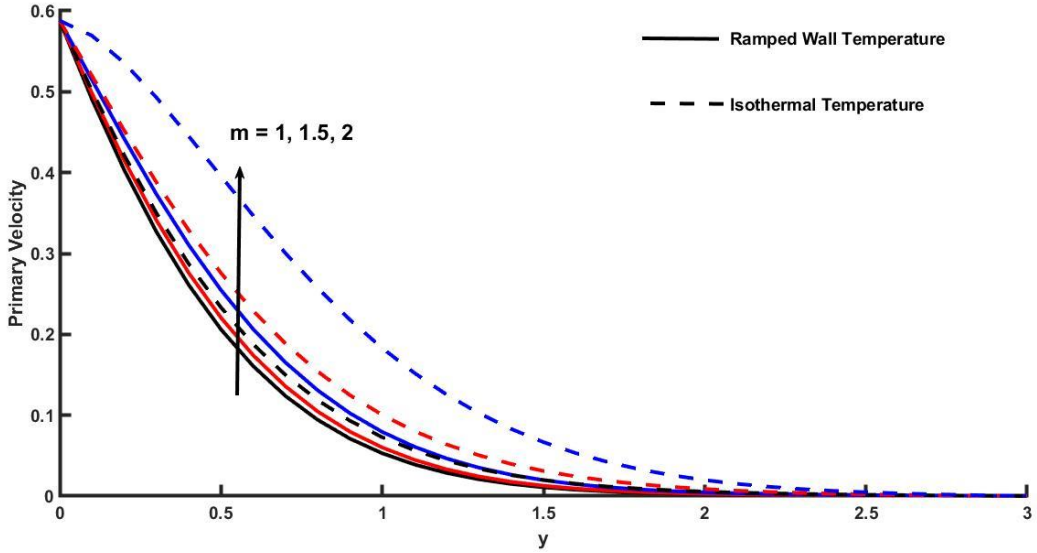

Figure 17: u on various weights of m

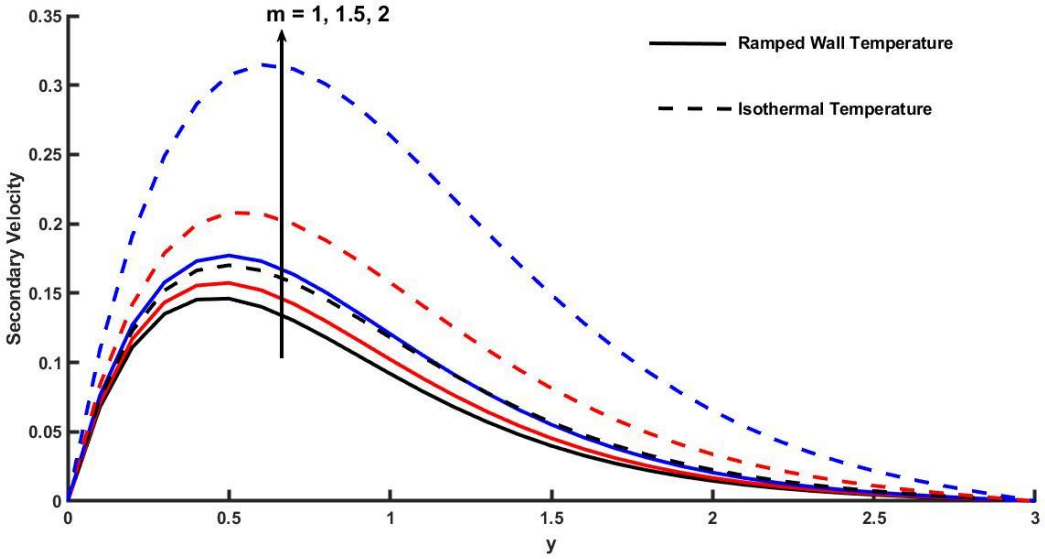

Figure 18: w on various weights of m

It is observed from the graphs that, for both thermal plates, u, w, T and C profiles acquire a specific most value close to floor of the plate after which lower as it should be on growing values of y to reach free flow position. It can be clearly seen that the u and w are better withinside the plate of isothermal as compare to the plate ramped temperature.

The Graphs 2 and 3 shows the effects of γ on u and w for both the plates. Its found that Primary moment getting down with growth in Casson fluid parameter all through the outer layer region, while Secondary moment to start with increase then lower down with growth in γ. The yield stress drops as the Casson parameter γ rises, which neglects the velocity outer layer thickness. The Casson fluid tends to decrease fluid velocity in x' direction because of the fluid's

versatility. Figures 4 and 5 shows how the first and second velocities of the fluid are influenced by M. u and w for both thermal plates reduces as M grows. This is because the fluid in the boundary layer experiences a resistive Lorentz force effect, which slows down the fluid's velocity. Drawing the curves of u and w for different weights of the permeability parameter k_1 with retaining the other parameters fixed is displayed in Figures 6 and 7. The k_1 helps to enhance the fluid's movement in both directions for both thermal plates. The physical circumstance whereby porosity increases is explained by a boost in boundary layer thickness and primary and secondary velocities. The impact of k on the u and w appears in Figures 8 and 9, they shows that the u declines with rising k across the outer surface for both the temperature, but k have a favourable effect on secondary fluid velocity. This suggests that k -rotation parameter impacts to slow down the flow of fluid in major directions(u) of flow for both thermal plates, whereas circular movement of the plate improves the secondary velocity of the flow. This is justified by the fact that rotation produces Coriolis force, which declines first velocity profile but improves the second velocity profile. Figure 10 shows that the θ going down with the increasing values of Pr and from graph 11 it is clear that the C and Schmidt number (Sc) are negatively correlated to each other. The influence of Kr on C is seen in graph 12. It is observed that concentration tends to decrease throughout the flow field due to chemical reaction. From Figure 13 and 14, we can observe that the Mass Grashof number (Gm) have the positive impact on the u and w. Figure 15 and 16 explains that the First and second velocity profile are positively correlated with the Gr. For ramping and isothermal temperature, the impact of m on u and w is shown in figures 17 and 18. It shows that across the outer surface region, first velocity and second velocity are rises as Hall current m increases. This indicates that Hall current helps to increase velocity of flow in either directions for both thermal plates. In the considered region, Hall current physically helps to produce secondary flow. We note that secondary flow is greater than primary flow as a result of this effect and the observations from figures 17 and 18. Additionally, it is observed that, in contrast to ramping boundary conditions, primary and secondary velocities are higher at isothermal temperature.

6. Conclusion

The main points that are reviled are listed below:

- The impact of all physical parameters have same behaviour for both the said temperatures.
- From the graphs, its clearly noticed that for all the physical parameter like u and w, temperature profile and concentration profile, etc., that the ramped temperature is always less than the isothermal temperature.
- Throughout the flow, the terms Hall current effect, the porous medium's permeability, thermal radiation and production of heat helps to intensify the primary as well as secondary velocity profile of the fluid
- Heat production and radiation from thermal sources are helping to improve the process heat transfer.
- Chemical reaction lower down the concentration profile.

Appendix:

$a = 1 + \frac{1}{\gamma}$	$a_1 = \frac{M^2(1-im)}{1+m^2} + \frac{1}{k_1} - 2ik^2$	$a_2 = \frac{1}{Pr}$

$a_3 = \frac{1}{Sc}$	$a_4 = \frac{a}{a_2} - 1$	$a_5 = a_1$
$a_6 = \frac{a_5}{a_4}$	$a_7 = \frac{Gr}{a_4}$	$a_8 = \frac{a}{a_3} - 1$
$a_9 = \frac{a\,Kr}{a_3} - a_1$	$a_{10} = \frac{a_9}{a_8}$	$a_{11} = \frac{Gm}{a_8}$
$a_{12} = -\frac{a_7}{a_6}$	$a_{13} = \frac{a_7}{{a_6}^2}$	$a_{14} = \frac{a_7}{(1-a_6)} - a_{12} - \frac{a_{13}}{(1-a_6)}$
$a_{15} = \frac{a_{11}}{a_{10}}$	$a_{16} = \frac{a_{11}}{{a_{10}}^2}$	$a_{17} = \frac{a_{11}}{(1+a_{10})} - a_{15} - \frac{a_{16}}{(1+a_{10})}$

References:

[1] N. Casson, A flow equation for the pigment oil suspensions of the printing ink type, in: Rheology of Disperse Systems, Pergamon, NewYork, (1959)84-102.
[2] M. Siva Sankari, M. Eswara Rao, Waris Khan, Mansoor H. Alshehri, Sayed M. Eldin, Shahid Iqbal, Analytical analysis of the double stratification on Casson nanofluid over an exponential stretching sheet, Case Studies in Thermal Engineering, Volume 50, October 2023, 103492.
[3] N. M. Hafez, Esraa N. Thabet, Zeeshan Khan, A. M. Abd-Alla, S. H. Elhag, Electroosmosis-modulated Darcy–Forchheimer flow of Casson nanofluid over stretching sheets in the presence of Newtonian heating, Case Studies in Thermal Engineering, Volume 53, January 2024, 103806.
[4] Prosanjit Das, Sarifuddin, Mainul Haque, Prashanta Kumar Mandal, Unsteady solute transport in Casson fluid flow and its retention in an atherosclerotic wall, Physica D: Nonlinear Phenomena, Volume 460, April 2024, 134094.
[5] Umar Farooq, Hassan Waqas, Sharifah E.Alhazmi, Abdullah Alhushaybari, Muhammad Imran, R. Sadat, Taseer Muhammad, Mohamed R. Ali, Numerical treatment of Casson nanofluid Bioconvectional flow with heat transfer due to stretching cylinder/plate: Variable physical properties, Arabian Journal of Chemistry, Volume 16, Issue 4, April 2023, 104589.
[6] P. Nagarani, Victor M. Job, P. V. S. N. Murthy, The effect of peristalsis on dispersion in Casson fluid flow, Ain Shams Engineering Journal, Available online 20 March 2024, 102758.
[7] Vidya Shree R., Patil Mallikarjun B., Kumbinarasaiah S., Entropy generation on an MHD Casson fluid flow in an inclined channel with a permeable walls through Hermite wavelet method, Results in Control and Optimization, Volume 12, September 2023, 100261.
[8] Afraz Hussain Majeed, Rashid Mahmood, Hasan Shahzad, Amjad Ali Pasha, Z. A. Raizah, Hany A. Hosham, D. Siva Krishna Reddy, Muhammad Bilal Hafeez, Heat and mass transfer characteristics in MHD Casson fluid flow over a cylinder in a wavy channel: Higher-order FEM computations, Case Studies in Thermal Engineering, Volume 42, February 2023, 102730.
[9] H. A. Ogunseye, S. O. Salawu, E. O. Fatunmbi, A numerical study of MHD heat and mass transfer of a reactive Casson–Williamson nanofluid past a vertical moving cylinder, Partial Differential Equations in Applied Mathematics, Volume 4, December 2021, 100148.

[10] N. M. Hafez, A. M. Abd-Alla, T. M. N. Metwaly, Influences of rotation and mass and heat transfer on MHD peristaltic transport of Casson fluid through inclined plane, Alexandria Engineering Journal, Volume 68, 1 April 2023, Pages 665-692.
[11] Dharmendar Reddy Yanala, M. Anil Kumar, Shankar Goud Bejawada, Kottakkaran Sooppy Nisar, R. Srinivasa Raju, V. Srinivasa Rao, Exploration of heat and mass transfer on 3-D radiative MHD Casson fluid flow over a stretching permeable sheet with chemical reaction, Case Studies in Thermal Engineering, Volume 51, November 2023, 103527.
[12] Dharmendar Reddy Yanala, Shankar Goud Bejawada, Kottakkaran Sooppy Nisar, Influence of Chemical reaction and heat generation/absorption on Unsteady magneto Casson Nanofluid flow past a non-linear stretching Riga plate with radiation, Case Studies in Thermal Engineering, Volume 50, October 2023, 103494.
[13] B. V. Swarnalathamma, D. M. Praveen Babu, M. Veera Krishna, Combined impacts of Radiation absorption and Chemically reacting on MHD Free Convective Casson fluid flow past an infinite vertical inclined porous plate, Journal of Computational Mathematics and Data Science, Volume 5, December 2022, 100069.
[14] Jawad Raza, Thermal radiation and slip effects on magnetohydrodynamic (MHD) stagnation point flow of Casson fluid over a convective stretching sheet, Propulsion and Power Research, Volume 8, Issue 2, June 2019, Pages 138-146.
[15] Majid Hussain, Abdul Ghaffar, Akhtar Ali, Azeem Shahzad, Kottakkaran Sooppy Nisar, M. R. Alharthi, Wasim Jamshed, MHD thermal boundary layer flow of a Casson fluid over a penetrable stretching wedge in the existence of nonlinear radiation and convective boundary condition, Alexandria Engineering Journal, Volume 60, Issue 6, December 2021, Pages 5473-5483.
[16] Dzuliana Fatin Jamil, Salah Uddin, Mohsin Kazi, Rozaini Roslan, M. R. Gorji, Mohd Kamalrulzaman Md Akhir, MHD blood flow effects of Casson fluid with Caputo-Fabrizio fractional derivatives through an inclined blood vessels with thermal, radiation, Heliyon, Volume 9, October 2023, e21780.
[17] Md. Yousuf Ali, Sk. Reza-E-Rabbi, Sarder Firoz Ahmmed, Md Nurun Nabi, Abul Kalam Azad, S.M. Muyeen, Hydromagnetic flow of Casson nano-fluid across a stretched sheet in the presence of thermoelectric and radiation, International Journal of Thermofluids, Volume 21, February 2024, 100484.
[18] B. Narsimha Reddy, P. Maddileti, Casson nanofluid and Joule parameter effects on variable radiative flow of MHD stretching sheet, Partial Differential Equations in Applied Mathematics, Volume 7, June 2023, 100487.
[19] Nadeem Abbas, Wasfi Shatanawi, Fady Hasan, Zead Mustafa,Thermal analysis of MHD casson-sutterby fluid flow over exponential stretching curved sheet, Case Studies in Thermal Engineering, Volume 52, December 2023, 103760.
[20] Ahmed Refaie Ali, Khuram Rafique, Maham Imtiaz, Rashid Jan, Hammad Alotaibi, Ibrahim Mekawy, Exploring magnetic and thermal effects on MHD bio-viscosity flow at the lower stagnation point of a solid sphere using Keller box technique, Partial Differential Equations in Applied Mathematics, Volume 9, March 2024, 100601.
[21] N. S. Yousef, Ahmed M. Megahed, Nourhan I. Ghoneim, M. Elsafi, Eman Fares, Chemical reaction impact on MHD dissipative Casson-Williamson nanofluid flow over a slippery stretching sheet through porous medium, Alexandria Engineering Journal, Volume 61, Issue 12, December 2022, Pages 10161-10170.
[22] B. Prabhakar Reddy, P. M. Matao, J. M. Sunzu, A finite difference study of radiative mixed convection MHD heat propagating Casson fluid past an accelerating porous plate including viscous dissipation and Joule heating effects, Heliyon (2024), HLY 28591.

[23] Harshad R. Patel, Effects of cross diffusion and heat generation on mixed convective MHD flow of Casson fluid through porous medium with non-linear thermal radiation, Heliyon, Volume 5, Issue 4, April 2019, e01555.
[24] Dolat khan, Gohar Ali, Poom Kumam, Kanokwan Sitthithakerngkiet, Fahd Jarad, Heat transfer analysis of unsteady MHD slip flow of ternary hybrid Casson fluid through nonlinear stretching disk embedded in a porous medium, Ain Shams Engineering Journal, Volume 15, Issue 2, February 2024, 102419.